Research Square

Preprints are preliminary reports that have not undergone peer review.
They should not be considered conclusive, used to inform clinical practice,
or referenced by the media as validated information.

Case studies of comprehensive gas control method during fully mechanized caving of low permeability ultra-thick coal seams

Bangyou Jiang (jiangbangyou123@163.com)
Shandong University of Science and Technology https://orcid.org/0000-0001-7763-9329
Shitan Gu
Shandong University of Science and Technology
Yunliang Tan
Shandong University of Science and Technology
Guangchao Zhang
Shandong University of Science and Technology
Jihua Zhang
Huaiyin Institute of Technology

Case study

Keywords: low permeability ultra-thick coal seam, fully mechanized caving, gas sources, hydraulic fracturing, gas drainage

Posted Date: November 17th, 2020

DOI: https://doi.org/10.21203/rs.3.rs-108415/v1

License: This work is licensed under a Creative Commons Attribution 4.0 International License.
Read Full License

Abstract

Slicing fully mechanized caving mining now is a common high-efficiency mining method for ultra-thick coal seams. However, effective gas control has remained a difficulty in fully mechanized top-coal caving mining of low permeability ultra-thick coal seams. This study focused on mining of the #9-15 coal in Liuhuanggou Coal Mine, Xinjiang Province, China, and combined theoretical analyses and field test results for exploring comprehensive gas control methods for fully mechanized caving of low permeability ultra-thick coal seams. The No. (9-15)06 panel is a top slicing panel of the #9-15 coal with a mining height of 9 m, and the No. (4-5)02 goaf is located on the top of the panel. Through analysis, gas emissions in the No. (9-15)06 panel were mainly sourced from the coal wall, caving of top coal, goaf, and neighboring coal seams. A comprehensive gas control method based on source separation was proposed, which combined gas pre-drainage along the coal seam, high-position drilling on the top, pre-burial of pipes in the goaf, and pressure-balancing ventilation. Considering the poor gas pre-drainage effect for low permeability coal seams, the permeability of the coal seam was enhanced using hydraulic fracturing. According to coal seam and crustal stress distribution characteristics, the arrangement of the boreholes and backward segmented fracturing technology were designed. Field data show that coal underwent remarkable pre-fracturing under hydraulic fracturing. Mean gas pre-drainage from the boreholes was enhanced by nearly 4 times compared to the pre-hydraulic fracturing state. Finally, using the proposed comprehensive control method based on the gas sources, field tests were performed in the No. (9-15)06 panel. Field measurement data demonstrate that gas concentration in the return airflow fluctuated within a range of 0.05%~0.35%, i.e., gas concentration did not exceed the standard. The proposed gas control method can provide insightful reference for the other similar projects.

1 Introduction

Slicing fully mechanized mining proves to be a high-efficiency mining method for ultra-thick seams that has been extensively applied in China. However, most of China's coal fields feature high gas and low permeability.[1, 2] Ultra-thick seams with low permeability are generally poor in gas pre-drainage. When using fully mechanized mining methods, a great amount of gas is emitted from coal seams. The accumulation of high-concentrations of gas in fractures in the overlying strata of the goaf can easily trigger a serious accident, such as a gas explosion, which seriously threatens production safety in the mines.[3, 4] In order to achieve effective gas control during fully mechanized mining of low permeability ultra-thick coal seams, numerous attempts to developed useful gas drainage and discharge methods have been made.

Fan *et al.* focused on fully mechanized mining of ultra-thick mines in Tashan Mine and proposed the gas in the goaf of the panel can be controlled well by combining surface vertical drilling and high position gas drainage roadways.[5] However, for the mines with great burial depth, gas drainage by drilling a great number of vertical holes. According to the characteristics of longwall coal mining in Australia, Guo *et al.* proposed a gas drainage and discharge method for the goaf using horizontal drilling, which exhibited

favorable drilling performance during construction on the bottom of the roof fracturing zone.[6] Zhang *et al.* examined the fracture development rules for the roof when using high-dipping longwall coal caving and the related effect on gas drainage;[7] according to their results, they designed an optimal construction layer during high-position drilling for gas drainage and discharge from the No. 704 panel of Baojishan Mine. Liu *et al.* addressed gas accumulation in the upper corner of the goaf in a fully mechanized panel for tilted ultra-thick coal seams by pre-burying gas drainage and discharge pipes in the goaf. This technique was successfully applied in Wudong Mine.[8]

In the above studies, straight line construction was performed for gas drainage in both surface and underground drilling process. In recent years, directional drilling has provided a new means of gas drainage in coal mines. Using directional drilling, holes can be drilled in coal seams along a preset direction.[9] Taking Daning Mine, Shanzi, China, as an example, Lu *et al*. carried out directional drilling in coal seams for gas pre-drainage and achieved favorable results.[10] Li *et al*. proposed a new inverse π-type drilling mode for gas drainage and discharge, which can realize comprehensive gas control after it passes through the caving zone, fracture zone, and coal seams in the working face.[11] In contrast with traditional drilling, directional coal seam drilling exhibits a series of advantages, including strong adaptability, high drilling proportion, and favorable gas drainage efficiency, which is particularly suited to gas control in single coal seams. However, directional drilling sets high demands on the coal seams, i.e., the coal seam should be quite permeable.

For low permeability coal seams, drilling along the coal seam has poor gas drainage performance; therefore, some fracturing techniques are necessary for pre-fracturing and permeability enhancement of coal seams. Deep-hole loosening blasting is a common pre-fracturing and permeability enhancement technique for coal seams;[12, 13] however, the technique has certain shortcomings. The dynamic shock wave produced in deep-hole blasting can easily cause damage to the surrounding rocks in the tunnel and make controlling rock deformation more difficult. In addition, unreasonable deep-hole blasting schemes also trigger numerous accidents such as gas explosions as well as coal and gas outbursts. Many scholars performed a numerous studies and explored some methods for permeability enhancement coal seams, such as hydraulic fracturing.[14–16] Hydraulic fracturing refers to drilling holes in the coal followed by generating fractures in the enclosed holes by utilizing a high-pressure water as medium and overcoming tensile strength of the rock and crustal stress using hydraulic pressure.[17] After hydraulic fracturing, the initial fractures in the coal form and numerous secondary fractures are produced.[17] Gas transport channels can be increased while promoting the desorption of adsorbed gas, thereby leading an increase in coal permeability and range.[18, 19] In recent years, some scholars developed directional hydraulic fracturing and pulsed hydraulic fracturing techniques.[20, 21]

Effective gas control has always remained as a critical technical difficulty in fully mechanized caving mining of low permeability ultra-thick coal seams. As described above, many scholars have proposed numerous gas control methods and ideas and gained favorable results. In fully mechanized mining of low permeability ultra-thick coal seams, gas has a variety of sources and is significantly difficult to

control. Currently, one method addressing the control of multi-source gas in the working face is lacking. This study focused on the mining of #9–15 coal in Liuhuanggou Coal Mine, Changji City, Xinjiang Province, China, analyzed the gas source in the working face and investigated a comprehensive gas control method for fully mechanized top-coal caving mining in low permeability ultra-thick coal seams by combining theoretical analysis and field test results. Firstly, both mining and geological conditions of the mines were introduced, and the coal seam mechanical parameters and in-situ crustal stress were measured to provide basic data for the gas control scheme design. Next, the main gas sources in the No. (9–15) 06 panel were analyzed and a comprehensive gas control method based on the sources of gas was proposed. Considering that low permeability coal seams exhibited poor gas pre-drainage performance, coal seams were pre-fractured using hydraulic pressure to increase permeability. The hydraulic fracturing scheme and technology were designed and the pre-fracturing and permeability enhancement performance of the coal seams were verified through field measurements. Finally, the effectiveness and reliability of the proposed source-separation comprehensive gas control method was validated using long-term field tests. The proposed gas control concept and methods can provide useful reference for other similar projects.

2 Case Study

2.1 Mining and geological conditions

This study focused on Liuhuagou Coal Mine in Xinjiang, China. As shown in Fig. 1, the primary mineable coal seam in Liuhuanggou Coal Mine, with a mean thickness of 32.94 m and mean inclination angle of 24°, includes the No. 9 ~ 15 coal seams. The coal seam also has great hardness and undeveloped fractures. In addition, the measured gas content in the No. 9 ~ 15 coal seams was 3.85 m^3/t, gas pressure was 0.5 MPa, the permeability coefficient ranges from 0.011814 to 0.061668 $m^2/MPa^2 \cdot d$, and the attenuation coefficient of gas flow in the hole was 1.03 ~ 1.28 d^{-1}, suggesting a low permeability coal seam.

The No. 7 and No. 4–5 coal was also located above the No. 9 ~ 15 coal seam, whose mean thicknesses were 2.31 m and 7.18 m, respectively. To be specific, No. 7 coal was unrecoverable. Gas contents in No. 7 and No. 4–5 coal were 4.14 m^3/t and 3.5 m^3/t, respectively. The distance between No. 4–5 coal and No.7 coal was 1.85 m, and the distance between No. 7 coal and #9–15 coal was 20.95 m. Roof strata of #9–15 coal seam were mainly composed of siltstones and mudstones, as shown in Fig. 2.

This study next selected the No. (9–15)06 panel as the operating background, which was 60 m away from the No (9–15)04 goaf. North of the (9–15)06 panel is unmined coal. The No. (4–5)04 goaf is located on the inclined top of the north part and the No. (4–5)02 goaf was right above the No. (9–15)06 panel. The tailgate in the No. (9–15)06 panel is inside staggered the tailgate in the No. (4–5)02 panel with a distance 23 m, while the headgate in the No. (9–15)06 panel is inside staggered the headgate in the No. (4–5)02 panel with a distance 11 m. A slicing mining method is used for #9–15 coal extraction. In the No. (9–15) 06 panel, a fully mechanized longwall caving method was used for top slicing of #9–15

coal, with a mining height of 9 m and a mechanized mining height of 3 m. The strike length and the inclined length of the working face were 1045 m and 100 m, respectively.

2.2 Coal seam mechanical parameters

In order to measure the related mechanical parameters of the #9–15 coal seam, #9–15 coal samples were collected along the tailgate. Because of the significant sample thickness, coal samples were sliced into three layers, namely, the upper slice, the middle slice, and the lower slice. Coal samples were processed into standard cylindrical specimens with different sizes (Φ50mm × 100 mm and Φ50mm × 25 mm). Next, using a MTS815 electro-hydraulic servo rock tester, uniaxial compressive, tri-axial compressive, and Brazilian disk splitting tests were performed on the standard samples to acquire the related parameters, including uniaxial compressive strength σ_c, tensile strength σ_t, elasticity modulus E, Poisson's ratio υ, cohesive force C, and internal friction angle φ. Each test was repeated 5 times and averaged. Table 1 lists the mechanical parameters of #9–15 coal. The mean uniaxial compressive strength of #9–15 coal was 35.35 MPa, suggesting great coal seam hardness. On account of poor permeability, gas pre-drainage performance along the coal seam was far from ideal. Gas control during mining in the No. (9–15)06 panel is of crucial importance.

Table 1 Mechanical properties of #9-15 coal

Lithology	σ_c (MPa)	σ_t (MPa)	E (GPa)	υ	C (MPa)	φ (°)
9-15 coal upper	39.06	1.96	3.84	0.26	3.8	40
9-15 coal middle	35.44	2.04	3.79	0.21	4.4	41
9-15 coal lower	31.56	1.91	2.32	0.23	3.9	42
Average	35.35	1.97	3.29	0.23	4.03	41

2.3 In-situ measurement of crustal stress

In order to gain in-depth knowledge of the crustal stress distribution in Liuhuanggou Mine, in-situ measurements were performed. The measurement accuracy of in-situ stress is related to the selected method and sensors. In this study, using stress relief method, a CSIRO hollow inclusion stress gauge from Australia was used, which possesses numerous advantages including accuracy, reasonable distribution of numerous strain gauges, and a wide application range.

The selection of the measuring points should avoid the areas with complex geological structures and significant mining effects as far as possible. 5 measuring points of crustal stress were selected, as the arrangement displayed in Fig. 3. Table 2 lists the arrangement of the crustal stress measuring points and the boreholes.

Table 2 In-situ stress measurement points and borehole layout parameters

No.	Drilling depth (m)	Azimuth (°)	Elevation angle (°)	Depth (m)	Lithology
Ⅰ	12.8	331	5	346	Fine sandstone
Ⅱ	12.0	325	10	482	Fine sandstone
Ⅲ	10.0	328	5	448	Fine sandstone
Ⅳ	10.5	320	41	360	Siltstone
Ⅴ	10.6	50	41	405	Siltstone

Figure 4 displays the in-situ crustal stress measurement results in Liuhuanggou Mine, in which σ_H, $\sigma_{h,}$ and σ_V denote the maximum horizontal principal stress, minimum horizontal principal stress, and vertical principal stress, respectively. The dominate azimuth angles along the maximum and minimal horizontal principal stress directions were 230°and 140°, respectively. Figure 3 displays the crustal stress direction at each measuring point. Figure 5 displays the in-situ stress variation in Liuhuanggou Mine with the burial depth.

Figure 5 displays the stress field in Liuhuanggou Mine, from which we can observe that $\sigma_V \approx \sigma_H \approx \sigma_h$. In addition, the vertical stress is dominated the crustal stress field and various principal stresses increase with increasing burial depth. Overall, vertical principal stress was slightly smaller than the weight of the overlying strata per unit area. Using the least squares method, the regression equation between various main principal stresses and burial depth can be written as:

$$h = 16.7\sigma_v + 244, R^2 = 0.60,$$

$$h = 13.0\sigma_v + 302, R^2 = 0.50,$$

$$h = 18.3\sigma_v + 304, R^2 = 0.74.$$

2.4 Analysis of gas sources in the No. (9–15)06 panel

Scholars have reached a consensus regarding gas sources and believed that gas in the mining face was mainly emitted from coal walls, fallen coal, the goaf, and neighboring coal seams.[22] By analyzing the arrangement and the surrounding mining conditions, 4 main gas emission sources in the No. (9–15)06 working face were identified.

(1) Gas emission quantity from coal walls (Q_1)

When the working face moved forwards, fresh coal walls are exposed to the air, and pressure balance was broken after reliving the rock pressure. Due to the existence of a gas pressure gradient in the coal, gas was emitted along coal fractures and towards the working face.

(2) Gas emission quantity from top coal caving (Q_2)

Before the caving of top coal in the working face, the top coal was first fully broken under the combined action of supporting pressure and the supports, and the original gas pressure balance in the coal seam was broken during crushing of the top coal. Accordingly, the adsorbed gas in the coal in the stable state was converted into free gas, which was then emitted into the working face during top coal caving.

(3) Gas emission quantity from the goaf (Q_3)

Using the fully mechanized caving method, the recovery ratio in the No. (9–15)06 panel was approximately 85%, and a great amount of coal would be left in the goaf. Therefore, gas from the remaining coal was the main source of the emitted gas in the goaf. In addition, mining of the top layer of the #9–15 coal seam affected the bottom coal seam to be mined, and numerous fractures were generated, thereby emitting a great amount of gas.

(4) Gas emission quantity from the neighboring coal seams (Q_4)

As shown in Fig. 2, the #7 and #4–5 coal seams right above #9–15 coal also featured high gas content, which were 20.95 m and 22.8 m away from #9–15 coal seam. After mining of the No. (9–15)06 panel, the #7 and #4–5 coal seams were located in roof caving zone. The roof caving zone in the No. (9–15)06 panel was connected with the No. (4–5)02 goaf. The gas emitted from the #7 and #4–5 coal seams accumulated in the overlying strata of the goaf in the No. (9–15)06 panel.

In conclusion, total gas emission quantity from the No. (9–15)06 panel (Q) equaled to the sum of the gas emission quantities from above sources, i.e., $Q = Q_1 + Q_2 + Q_3 + Q_4$. Q_1 and Q_2 can be lowered by gas pre-drainage along the coal seams.[23] The gas from latter two sources accumulated in fractures in the overlying goaf strata. The friction during the breaking movement of the overlying strata easily triggered gas explosion accidents in the goaf, which seriously threatened production safety in the working face. Therefore, for the gas accumulated on the top of the goaf ($Q_3 + Q_4$), effective measures are required for drainage or dilution.

3 Enhancement Of Coal Seam Permeability Via Hydraulic Fracturing

On account of the high strength and poor permeability of the #9–15 coal seam, gas pre-drainage performance was poor. Therefore, pre-fracturing and permeability enhancement should be first performed on the coal seam via hydraulic fracturing for improving gas pre-drainage effect of the coal seam.

3.1 Crack initiation pressure

Crack initiation pressure (hereinafter referred to as the initiation pressure) refers to the maximum water pressure during hydraulic fracturing. Numerous factors including burial depth of the coal seam, crustal stress, coal mechanical properties, and original cracks can affect initiation pressure. According to hydraulic fracturing theory,[14, 24–26] tensile cracks dominate the hydraulic fracturing process. Under the action of water pressure in the boreholes and the crustal stress field, when the tensile stress on the tip of the cracks exceeds the tensile strength σ_t, cracks develop gradually. By ignoring the water seepage effect from the boreholes on the surrounding media, the initiation pressure can be estimated as [26]

$$P_{k1} \geq 3\sigma_3 - \sigma_1 + \sigma_t \quad (1)$$

where σ_1 denotes the maximum principal stress, σ_3 denotes the minimum principal stress, and σ_t denotes the coal tensile strength.

Additionally, gas pressure also significantly affects crack initialization and propagation under hydraulic fracturing.[27] Based on statistics from a large number of coal mines in China, Li *et al*. carried out regression analysis and determined the following relationship between crack initialization pressure P_{k2}, burial depth of the coal seam H, and gas pressure P_0: [19]

$$P_{k2} = 0.023H + 1.293P_0 + 2.04 \quad (2)$$

According to the minimum pressure principle, the minimum value between P_{k1} and P_{k2} was selected as the initialization pressure of the coal seam (P_k):

$$Pk = \min\{P_{k1}, P_{k2}\} \quad (3)$$

In this study, mean burial depth of the working face was approximately 420 m, mean unit weight of the overlying strata was 23 kN/m^3, and gas pressure of the coal seam was 0.5 Mpa. According to measurements, the maximum principal stress and minimum principal stress in the test region were 10.54 MPa and 6.34 MPa, respectively, through inversion. The average tensile strength of #9-15 coal was 1.97 MPa (Table 1). Therefore, P_{k1}= 10.45 MPa and P_{k2}=10.74 Mpa. According to Eq. (3), P_k=10.45 MPa.

3.2 Coal seam permeability enhancement via hydraulic fracturing

(1) Arrangement of hydraulic fracturing boreholes

Based on engineering and geological conditions of the No. (9–15)06 panel and coal seam occurrence characteristics, the spatial positions of the hydraulic fracturing boreholes and high-position gas drainage

boreholes on the roof of the working face were analyzed to avoid damages to gas drainage boreholes. Figure 6 displays the arrangement of hydraulic fracturing boreholes.

A set of boreholes with a diameter of 75 mm were arranged on the inner sides of tailgate and headgate. The first group boreholes was arranged 15 m from the set-up room of the No. (9–15)06 panel, and the interval between every two groups of boreholes is 8 m. Table 3 lists the detailed parameters of the boreholes.

Table 3 Detailed borehole parameters

Location	Number	Dip angle/°	Diameter/mm	Length/m	Height of the orifice from the floor of roadway /m
Tailgate	1#	12	75	11	1.5
	2#	0	75	17	1.0
	3#	-11	75	34	0.5
Headgate	4#	30	75	60	1.5
	5#	34	75	35	1.8
	6#	43	75	19	2.1

(2) Field equipment for hydraulic fracturing included a high-pressure water-injection pump, water tank, flow controller, pressure gauge, and high-pressure water pipes. The maximum water injection pressure of the water injection pump was 35 MPa, and the water flow velocity was 200 L/min.

(3) Sealing of boreholes

Borehole sealing is a critical make-or-break step that determines the effectiveness of hydraulic fracturing. Currently, people always use cement and other special hole packers for sealing.[19] The latter was used in the present field test. Under high-pressure water, the rubber gasket in the hole packer was compressed, then expanded radially and reached the inner wall of the hole to achieve a seal. Using this method, borehole sealing efficiency was high and the whole operating process was simple. However, this process set high requirements on the boreholes, i.e., the construction quality should be high and the borehole wall should be smooth.

(4) Fracturing technology

Spatial propagation characteristics of the hydraulic fractures directly affect permeability enhancement effect of the coal seam. The hydraulic fractures always propagated along the direction parallel to the maximum principal stress and perpendicular to the minimum principal stress.[17, 28, 29]

According to in-situ measurement results, vertical stress dominated the crustal stress field in Liuhuanggou Mine, and the dominant angle of the minimum horizontal principal stress was 140°, i.e., the

angle between dominant direction of the minimum horizontal principal stress and the gate axis of the panel was approximately 84°. Hydraulic fractures in the boreholes are more likely to propagate radially from the borehole; therefore, in order to enhance hydraulic fracturing performance, backward segmented fracturing technology was adopted. Figure 7 illustrates the present borehole sealing method. Two hole packers were connected in series, and the spacing distance between them (denoted as L) was the sectional fracturing length. In this study, L = 8 ~ 10 m. In Fig. 8, the opening pressure of the pressure valve in hole packer A equaled that in hole sealer B, and both were smaller than the opening pressure of pressure valve C. Accordingly, local borehole sealing and fracturing can be easily achieved.

3.3 Verification of permeability enhancement of the coal seam via hydraulic fracturing

In order to evaluate permeability enhancement performance of the coal seam under hydraulic fracturing, this study used the following two methods for verification—boroscope examination and borehole gas emission quantity measurement.

(1) Method 1: boroscope examination

A stratum detector (Fig. 8) was employed for examining fracturing results in the drilling hole before and after hydraulic fracturing. Both crack initiation and propagation behaviors in the holes were the research emphasis in this study. Figure 9 displays the distribution of cracks in the borehole before and after hydraulic fracturing. The inner wall of the initial borehole was very complete in shape while few original cracks were found in the borehole. After hydraulic fracturing, cracks mainly propagated radially from the borehole wall or in spiral pattern along the borehole wall, which correlates with the distribution of crustal stress in the test region, which was consistent with the predicted results as described above. In conclusion, the coal seam showed satisfactory pre-fracturing performance.

(2) Method 2: Measurement of gas emission quantity from the borehole

Gas pre-drainage flows before and after hydraulic fracturing were monitored using an orifice plate flowmeter.[30] The gas flow in the borehole can be calculated as:

$$Q_m = kb\sqrt{\Delta h}\delta_p\delta_T \quad (4)$$

$$Q_c = Q_m X \quad (5)$$

where Q_m denotes the flow of drained gas mixture, with units of m^3/min; Q_c denotes the flow of drained pure gas, with units of m^3/min; X denotes gas concentration in the gas mixture, with units of %; b denotes the correction coefficient of gas concentration ($b = \sqrt{1/(1-0.00446X)}$); Δh denotes the measured pressure difference between the front and the rear ends of the hole plate, with units of mmH_2O; δ_p denotes the correction coefficient of gas pressure ($\delta_p = \sqrt{P_T/760}$, in which 760 is the standard atmospheric pressure and P_T denotes the measured absolute pressure at the windward end of the hole plate, with units of mmHg); δ_T denotes the correction coefficient of temperature ($\delta_T = \sqrt{293/(273+t)}$, in which 293 is the standard absolute temperature and t denotes the temperature at the measuring point in the gas pipe, with units of °C); k denotes actual characteristic coefficient of orifice flow.

The readings from the U-shaped differential pressure gauge were obtained and substituted into Eq. (4) and Eq. (5) for calculating the exhausted gas mixture and pure gas. According to field test results, the variation rules of gas pre-drainage quality from a single borehole with time before and after hydraulic fracturing were plotted (Fig. 10).

It can be observed from Fig. 10 that after the implementation of hydraulic fracturing, mean gas pre-drainage quantity from the borehole was enhanced by nearly 4 times the original value. In addition, for low permeability hard coal from Liuhuanggou Mine, fractures in the coal around the borehole were propagated after hydraulic fracturing, thereby enhancing the permeability of the surrounding coal seams and remarkably improving gas pre-drainage performance.

4 Comprehensive Gas Control Based On Sources

By analyzing four main gas emission sources in the No. (9–15)06 panel, a comprehensive gas control method based was proposed (Fig. 11). Before mining in the panel, the gas emission quantity from the coal wall (Q_1) and the gas emission quantity form top coal caving (Q_2) were lowered by performing gas pre-drainage along the coal seam. During mining of the working face, the gas accumulated in the caving zone and the fracture zone ($Q_3 + Q_4$) was discharged via high-position boreholes on the roof. Meanwhile, drainage pipes were buried along the tailgate in the panel to address the accumulation of gas in the upper corner. Additionally, pressure-balancing ventilation was implemented during mining. The pressure

difference between the two gate roads was reduced by adjusting the ventilation parameters to reduce air leakage and gas emissions in the goaf.

(1) Gas pre-drainage along the coal seam

Hydraulic fractured boreholes were also used as gas pre-drainage holes before the mining in the panel for gas pre-drainage along the coal seam (Fig. 12). Accordingly, a hole achieved two purposes—enhancement of gas pre-drainage and reduction of construction volume.

The gas pre-drainage system along the coal seam mainly consisted of drainage pipe, filter pipe, collecting pipe, and hole-sealing materials (Fig. 12). The auxiliary devices mainly included the flowmeter, the concentration meter, and the pressure gauges. Metal sleeves with a diameter of 40 mm and a wall thickness of 3 mm were put in each hydraulic fractured borehole and some small-diameter holes were arranged on one end of the sleeves. Two sections of sleeves were arranged around each borehole, and each section was 3 ~ 4 m in length. After installation of the sleeves, boreholes were sealed using polyurethane (PU). It should be noted that hole-sealing depth should not exceed the burial depth of the gas drainage pipe in the borehole. Finally, the sleeves were connected with the gas drainage header pipes. The gas drainage head pipes provided a negative pressure of 25 kPa.

(2) Drainage of gas from the caving zone via high-position boreholes

Gas emitted from pressure relief in the coal seam floor was an important source of gas in the panel during mining. After the mining, the overlying strata underwent fracturing, finally forming the bent subsidence zone, the fracture zone, and the caving zone;[31–34] meanwhile, a great number of layered and vertical fractures were produced,[35, 36] and gas accumulated in these regions. Accumulation of the gas emitted from the #4–5 coal, the #7 coal and the #9–15 coal increased the possibility of gas accidents. Therefore, on the basis of gas pre-drainage along the coal seam before the mining, long-strike holes were drilled in the high-position drilling site on the roof for discharging the gas accumulated in the caving zone and the fracture zone during mining (Fig. 13). The high-position drilling site was located in the tailgate of the No. (9–15)06 panel. Drilling sites were set at an interval of 60 m. In each drilling site, 16 long boreholes in 4 rows were arranged along the strike of the coal seam in a fan-shaped distribution.

(3) Gas drainage at the upper corner of the panel

The gas produced in pressure relief from the floor can rush into the goaf and enter the upper corner, which can result in an abundance of gas in the corner. In order to avoid above problem, gas drainage pipes were buried at the air return corner on the top of the goaf during mining, which assists gas drainage in the goaf (Fig. 13).

(4) Pressure-balancing ventilation for reducing air leakage in the goaf

People generally increased the air supply for diluting the gas concentration in the return airflow for the panels with U-shaped ventilation. Unfortunately, it is an incorrect practice. Increasing air supply quantity

in the panel blindly can increase the air pressure difference between the goaf and the panel as well as air leakage in the panel, leading to an increase in gas emission in the goaf and gas concentration in the return airflow.[37] On that basis, pressure-balancing ventilation[38] was adopted to reduce the pressure difference between two sides in both the air intake and return roadways and changing the pressure distribution in the ventilation system. Accordingly, air leakage in the goaf can be lowered to inhibit gas emission from the upper corner of the goaf.

4.5 Analysis of gas comprehensive control effect

Finally, a long-term filed test was performed in the No. (9–15)06 panel using the comprehensive control method based on the sources of gas. Overall, gas was adequately controlled. Figure 14 displays the monitoring gas concentrations in the panel during the mining period. The gas concentration in the return airflow fluctuated within a range of 0.05%~0.35%, and the maximum gas concentration was no greater than 0.35%, which is far below the early warning value 0.5%.

5 Conclusions

Gas control has always been a key problem during slice mining of ultra-thick coal seams with high gas content. This study examined the No. (9–15)06 panel in Liuhuanggou Coal Mine. The #9–15 coal seam, with a mean thickness of 32.94 m, included low permeability ultra-thick coal seams with high gas content. The No. (9–15)06 panel is the top slicing working face of #9–15 coal, which uses fully mechanized top coal caving with a mining height of 9 m. A large amount of gas was emitted from the panel during mining.

Based on the arrangement in the No. (9–15)06 panel and the surrounding mining condition, gas in the panel had four emission sources—gas emission from the coal wall, gas emission from top coal caving, gas emission from the goaf, and gas emission from the neighboring coal seams. Gas emitted during mining easily accumulated in the fractures in the overlying goaf, which posed great threat to production safety in the panel. Therefore, a comprehensive control method based on the sources of gas for the panel was proposed in this study. Before mining, gas emissions from the coal walls and top coal caving were lowered via gas pre-drainage along the coal seam. After mining, gas accumulated in the caving zone and the fracturing zone was drained by using long-strike boreholes in the high-position drilling site. Drainage pipes were buried in the upper corner of goaf to avoid gas accumulation emitted from de-stressed floor coal seams. During mining, by means of pressure-balancing ventilation, air leakage in the goaf and gas emission from the goaf can be reduced.

Due to the great hardness and poor permeability of the #9–15 coal seam, conventional gas pre-drainage methods along the seam do not perform well. This study enhanced the permeability of the coal seam via hydraulic fracturing. Based on the measured results of crustal stress, the crack initiation pressure of the #9 ~ 15 coal seam under hydraulic fracturing was 10.45 MPa, and the arrangement scheme of the boreholes for hydraulic fracturing in the coal seam was designed. According to the measured crustal

stress field, it was predicted that hydraulic fractures were more likely to propagate radially from the borehole. Backward segmented hydraulic fracturing technology was designed for improving hydraulic fracturing performance. In order to validate the superiority of the proposed method, the pre-fracturing performance of the coal seam was evaluated using boroscope examination and gas emission tests. Field test results demonstrate that after hydraulic fracturing, obvious fracture development can be observed in the coal around the boreholes. Fractures mainly initiated radially from the hole wall and then propagated along the hole wall in spiral pattern, which was consistent with crustal stress measurements. After hydraulic fracturing, mean gas pre-drainage was enhanced by nearly 4 times.

Finally, a long-term field test was performed in the No. (9–15) panel to validate the superiority of the proposed comprehensive control method based on the gas sources. Long-term monitoring results indicate that gas concentration in the return airflow fluctuated within a range of 0.05%~0.35%. No warning of excessive gas appeared in the panel. Adequate gas control can effectively ensure mining safety in the panel.

Declarations

Acknowledgements

This research is supported by the National Key Research and Development Program of China (2018YFC0604703), the Natural Science Foundation of Shandong Province, China (ZR2019BEE001, ZR2018MEE009) and Scientific Research Foundation of Shandong University of Science and Technology for Recruited Talents (2017RCJJ012). The authors thank the anonymous referees for their careful reading of this paper and valuable suggestions.

References

1 Yang XL, Wen GC, Sun HT, Li XL, Lu TK, Dai LC, Cao J, Li L. Environmentally friendly techniques for high gas content thick coal seam stimulation—multi-discharge CO2 fracturing system. *J Nat Gas Sci Eng*. 2019; 61: 71-82.

2 Xia TQ, Zhou FB, Liu JS, Gao F. Evaluation of the pre-drained coal seam gas quality. *Fuel*. 2014; 130: 296-305.

3 Jiang FX, Kong LH, Liu CG. Gas emission laws of fully-mechanized sublevel caving mining in extra-thick coal seam. *J China Coal Soc*. 2011; 36(03): 407-411.

4 Wang W, Cheng YP, Wang HF, Liu HY, Wang L, Li W, Jiang JY. Fracture failure analysis of hard–thick sandstone roof and its controlling effect on gas emission in underground ultra-thick coal extraction. *Eng Fail Anal*. 2015; 54: 150-162.

5 Duan YP, Wang YB. Study on measures to control methane in goaf in mechanized mining extremely thick face of Tashan coal mine. *China Safety Sci J*. 2016; 26(12): 116-121.

6 Guo H, Todhunter C, Qu QD, Qin ZY. Longwall horizontal gas drainage through goaf pressure control. *Int J Coal Geol*. 2015; 150-151: 276-286.

7 Zhang Y, Zhang B, Li L, Zhang SQ, Liu JK, Zhao JJ. Study on the effect of roof fracture development on gas drainage in steep full-mechanized caving mining. *J Min Safety Eng*. 2014; 31(05): 809-813.

8 Liu ZQ. Gas drainage effect analysis of buried pipes in steeply inclined thick coal seam fully-mechanized caving face. *Coal Sci Tech*. 2017; 45(S1): 74-76.

9 An FH, Wang ZF, Yang HM, Yang SY, Pan FM, Chen T, Xie C. Application of directional boreholes for gas drainage of adjacent seams. *Int J Rock Mech Min Sci*. 2016; 90: 35-42.

10 Lu SQ, Cheng YP, Ma JM, Zhang YB. Application of in-seam directional drilling technology for gas drainage with benefits to gas outburst control and greenhouse gas reductions in Daning coal mine, China. *Nat Hazards*. 2014; 73(3): 1419-1437.

11 Li YK, Wu SY, Nie BS, Ma YK. A new pattern of underground space-time tridimensional gas drainage: A case study in Yuwu coal mine, China. *Energy Sci Eng*. 2019; 7(2): 399-410.

12 Liu J, Liu ZG, Gao K, Jiang EL. Application of deep borehole blasting to top-coal pre-weakening and gas extraction in fully mechanized caving. *Chin J Rock Mech Eng*. 2014; 33: 3361-3367.

13 Zhu WC, Wei CH, Li S, Wei J, Zhang MS. Numerical modeling on destress blasting in coal seam for enhancing gas drainage. *Int J Rock Mech Min Sci*. 2013; 59: 179-190.

14 Bohloli B, de Pater CJ. Experimental study on hydraulic fracturing of soft rocks: Influence of fluid rheology and confining stress. *J Petrol Sci Eng*. 2006; 53: 1-12.

15 Yan CZ, Zhang H, Sun GH, Ge XR. A 2d fdem-flow method for simulating hydraulic fracturing. *Chin J Rock Mech Eng*. 2015; 1: 67-75.

16 Lockner D, Byerlee JD. Hydrofracture in Weber Sandstone at high confining pressure and differential stress. *J Geophys Res*. 1977; 82(14): 2018-2026.

17 Adachi J, Siebrits E, Peirce A, Desroches J. Computer simulation of hydraulic fractures. *Int J Rock Mech Min Sci*. 2007; 44(5): 739-757.

18 Zhai C, Li XZ, Li QG. Research and application of coal seam pulse hydraulic fracturing technology. *J China Coal Soc*. 2011; 36(12): 1996-2001.

19 Li Q, Lin B, Zhai C. A new technique for preventing and controlling coal and gas outburst hazard with pulse hydraulic fracturing: a case study in Yuwu coal mine, China. *Nat Hazards*. 2015; 75(3): 2931-2946.

20 Zhai C, Li M, Sun C, Zhang JG, Yang W, Li QG. Guiding-controlling technology of coal seam hydraulic fracturing fractures extension. *Int J Min Sci Tech*. 2012; 22(6): 831-836.

21 Li Q, Lin B, Zhai C. The effect of pulse frequency on the fracture extension during hydraulic fracturing. *J Nat Gas Sci Eng*. 2014; 21: 296-303.

22 Zhou W, Yuan L, Zhang GL, Du HL, Xue S, He GH, Han YC. A new method for determining the individual sources of goaf gas emissions: a case study in Sihe Coal Mine. *J China Coal Soc*. 2018; 43(04): 1016-1023.

23 Xing Y, Zhang F. Optimizing borehole spacing for coal seam gas pre-drainage. *J Geophys Eng*. 2019; 16(2): 399-410.

24 Rahman MK, Joarder AH. Investigating production-induced stress change at fracture tips: Implications for a novel hydraulic fracturing technique. *J Petrol Sci Eng* 2006; 51(3-4): 185-196.

25 Huang BX, Zhao XL, Chen SL, Liu JW. Theory and technology of controlling hard roof with hydraulic fracturing in underground mining. *Chin J Rock Mech Eng* 2017; 36(12): 2954-2970.

26 Hubbert MK, Willis DG. Mechanics of Hydraulic Fracturing. *In: Transactions of Society of petroleum engineers of AIME* 1957; 210: 153-168.

27 Lin BQ, Meng J, Ning J, Zhang MB, Li QG, Liu Y. Research on dynamic characteristics of hydraulic fracturing in coal body containing Gas. *J Min Safety Eng*. 2012; 29(01): 106-110.

28 Huang BX, Liu CY, Fu JH, Guan H. Hydraulic fracturing after water pressure control blasting for increased fracturing. *Int J Rock Mech Min Sci*. 2011; 48(6): 976-983.

29 Li Gen, Tang CA, Li LC, Liang ZZ. Numerical simulation of 3D hydraulic fracturing process. *Chin J Geot Eng*, 2010; 32(12): 1875-1881.

30 Cao YX, Zhang JS, Tian L, Zhai H, Fu GT, Tang JH. Research and application of CO^2 gas fracturing for gas control in low permeability coal seams. *J China Coal Soc*. 2017; 42(10): 2631-2641.

31 Jiang BY, Gu ST, Wang LG, Zhang GC, Li WS. Strainburst process of marble in tunnel-excavation-induced stress path considering intermediate principal stress. *J Cent South Univ*. 2019; 26(4): 984-999.

32 Wang J, Ning JG, Jiang JQ, Bu TT. Structural characteristics of strata overlying of a fully mechanized longwall face: a case study. *J S Afr I Min Metall*. 2018; 118: 1195-1204.

33 Wen ZJ, Xing ER, Shi SS, Jiang YJ. Overlying strata structural modeling and support applicability analysis for large mining-height stopes. *J Loss Prevent Proc*. 2019; 57: 94-100.

34 Liu XS, Tan YL, Ning JG, Lu YW, Gu QH. Mechanical properties and damage constitutive model of coal in coal-rock combined body. *Int J Rock Mech Min Sci*. 2018; 110: 140-150.

35 Guo WY, Tan YL, Yu FH, Zhao TB, Hu SC, Huang DM, Qin ZW. Mechanical behavior of rock-coal-rock specimens with different coal thicknesses. *Geomech Eng*. 2018; 15(4): 1017-1027.

36 Fang K, Zhao TB, Zhang YB, Qiu Y, Zhou JH. Rock cone penetration test under lateral confining pressure. *Int J Rock Mech Min Sci*. 2019; 119: 149-155.

37 Lin BQ, Zhou SN, Zhang RG. Methane controlling technique at the upper corner of the goaf in u- type ventilation face. *J China Coal Soc*. 1997; 22(5): 63-67.

38 Wang G, Wang R, Wu MM, Xin L, Zhou XH, Liu CW. Prevention and control technology of harmful gas intrusion in close-up coal seam under fire area. *J China Coal Soc*. 2017; 42(07): 1765-1775.

Figures

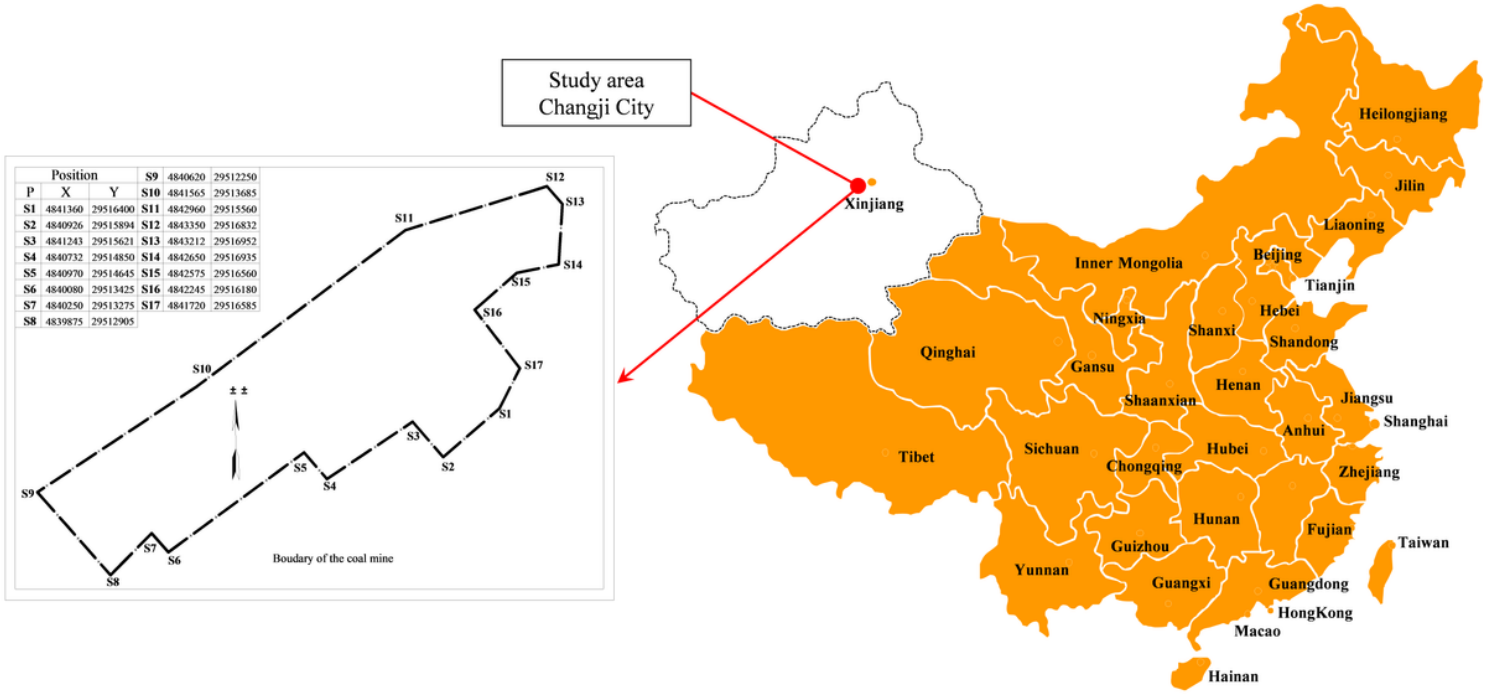

Figure 1

Location of the test site. Note: The designations employed and the presentation of the material on this map do not imply the expression of any opinion whatsoever on the part of Research Square concerning the legal status of any country, territory, city or area or of its authorities, or concerning the delimitation of its frontiers or boundaries. This map has been provided by the authors.

No.	Lithology	Column	Thickness (m)	Depth (m)	Remark
1	Siltstone		17.39	343.52	
2	Fine sandstone		2.89	346.41	
3	Carbonaceous mudstone		1.35	347.76	
4	4-5 coal seam		7.18	354.94	Coal
5	Siltstone		1.85	356.79	
6	7 coal seam		2.31	359.10	Coal
7	Mudstone		3.65	362.75	
8	Carbonaceous mudstone		2.23	364.98	
9	Fine sandstone		1.30	366.28	
10	Siltstone		11.46	377.74	
11	9-12 coal seam		13.51	391.25	Coal
12	Mudstone		0.90	392.15	
13	13-15 coal seam		19.43	411.58	Coal
14	Carbonaceous mudstone		5.76	417.34	
15	Siltstone		5.11	422.45	
16	Fine sandstone		9.17	431.62	

Figure 2

Stratigraphy column of test site

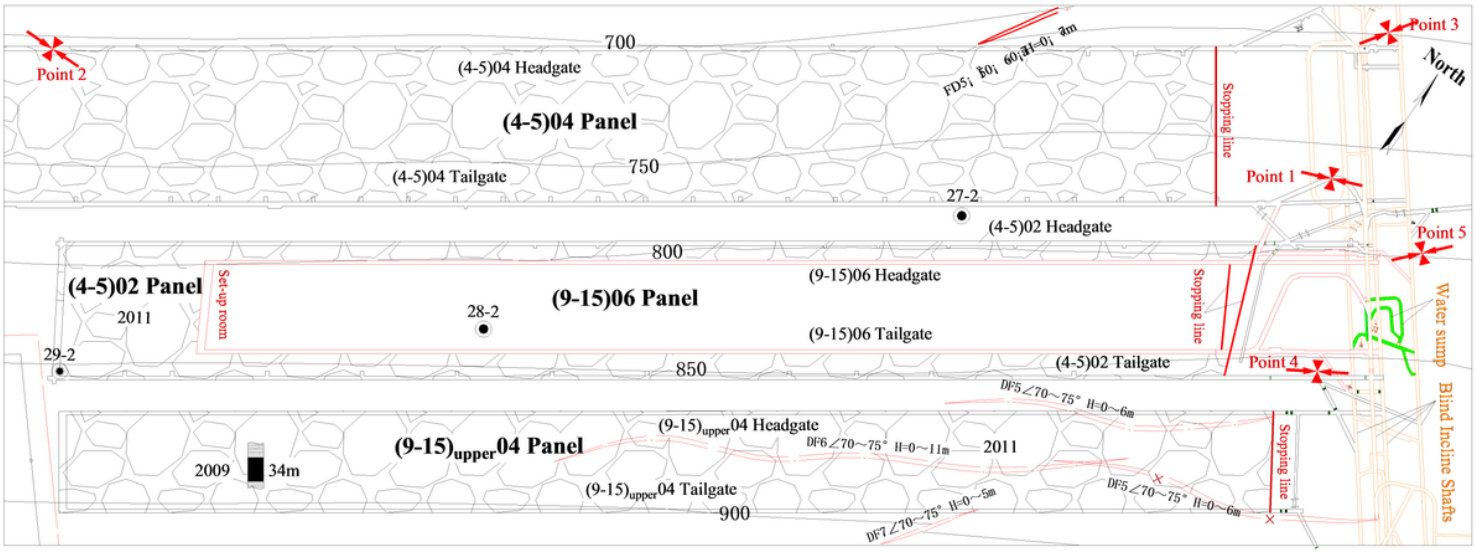

Figure 3

Layout of (9-15)06 panel

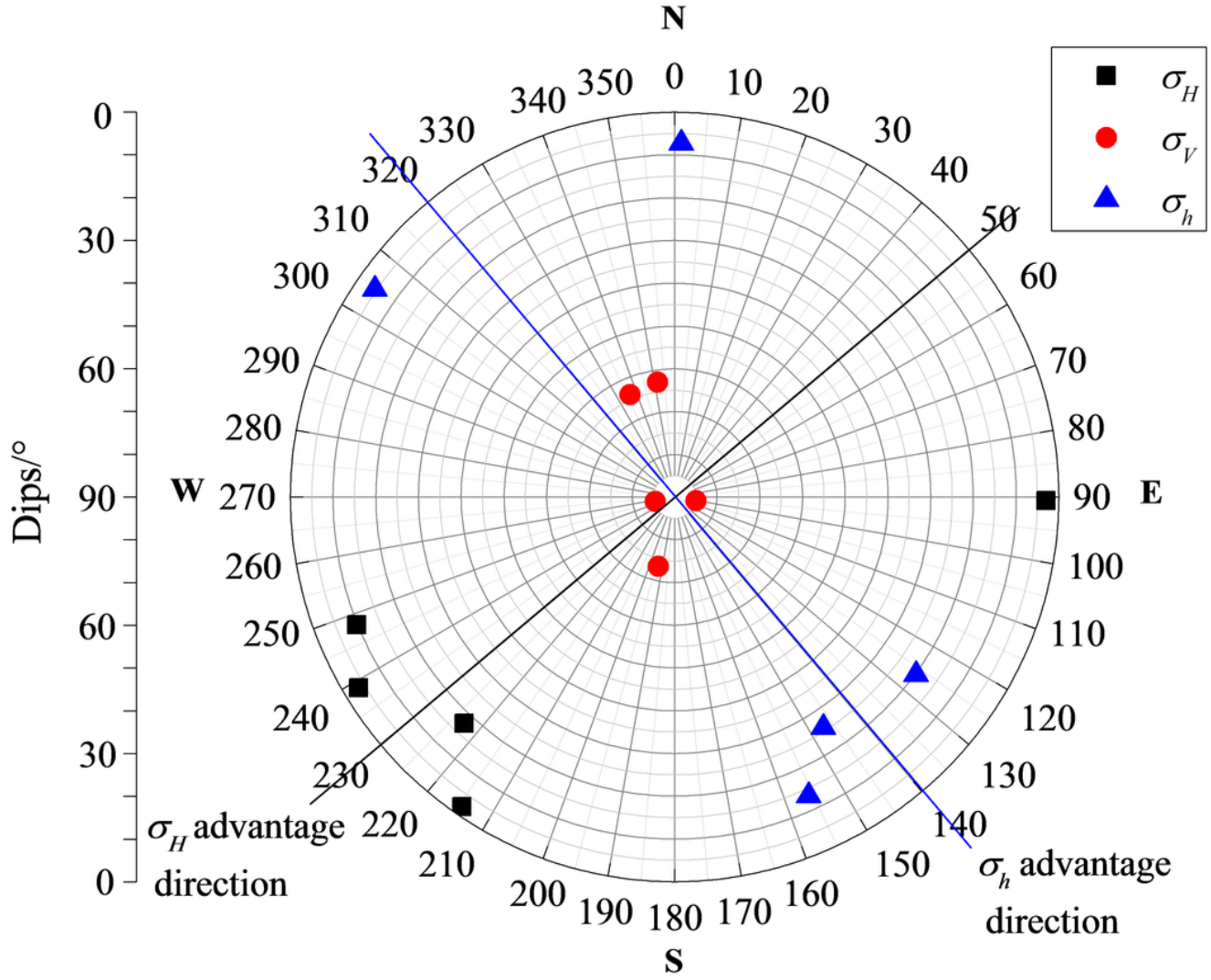

Figure 4

In-situ stress Direction of Liuhuanggou Coal Mine

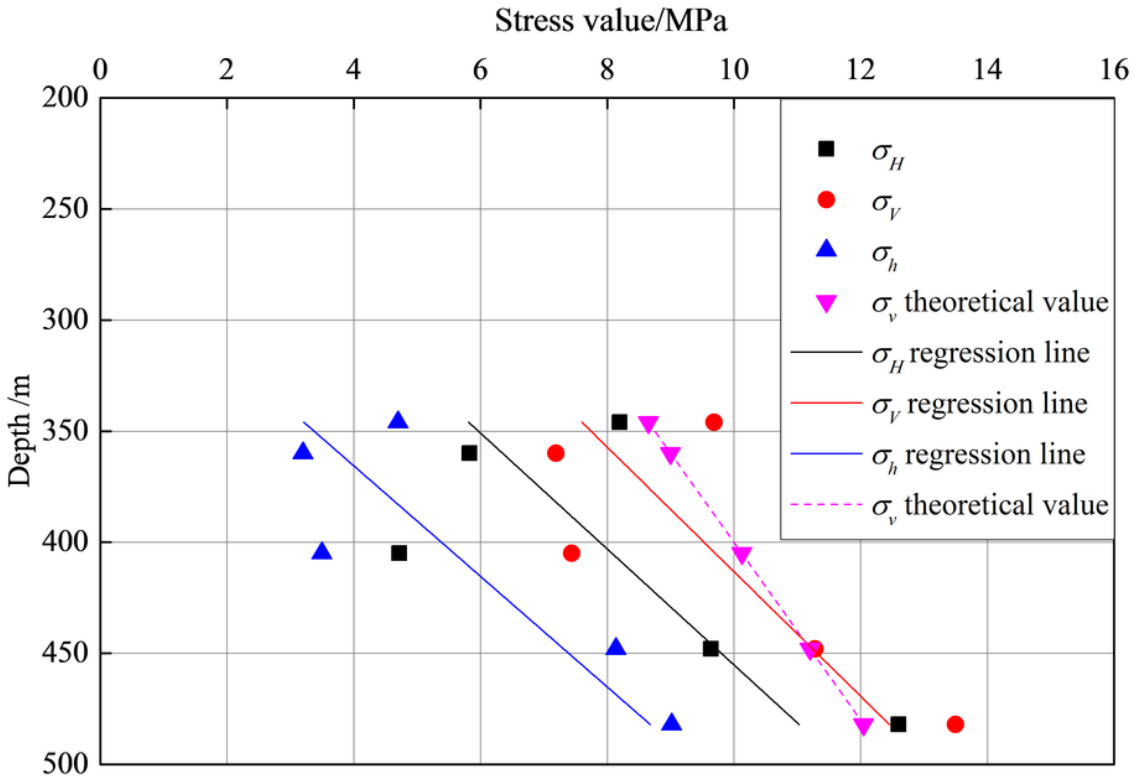

Figure 5

Relation between in-situ stress magnitude and depth of Liuhuanggou Coal Mine

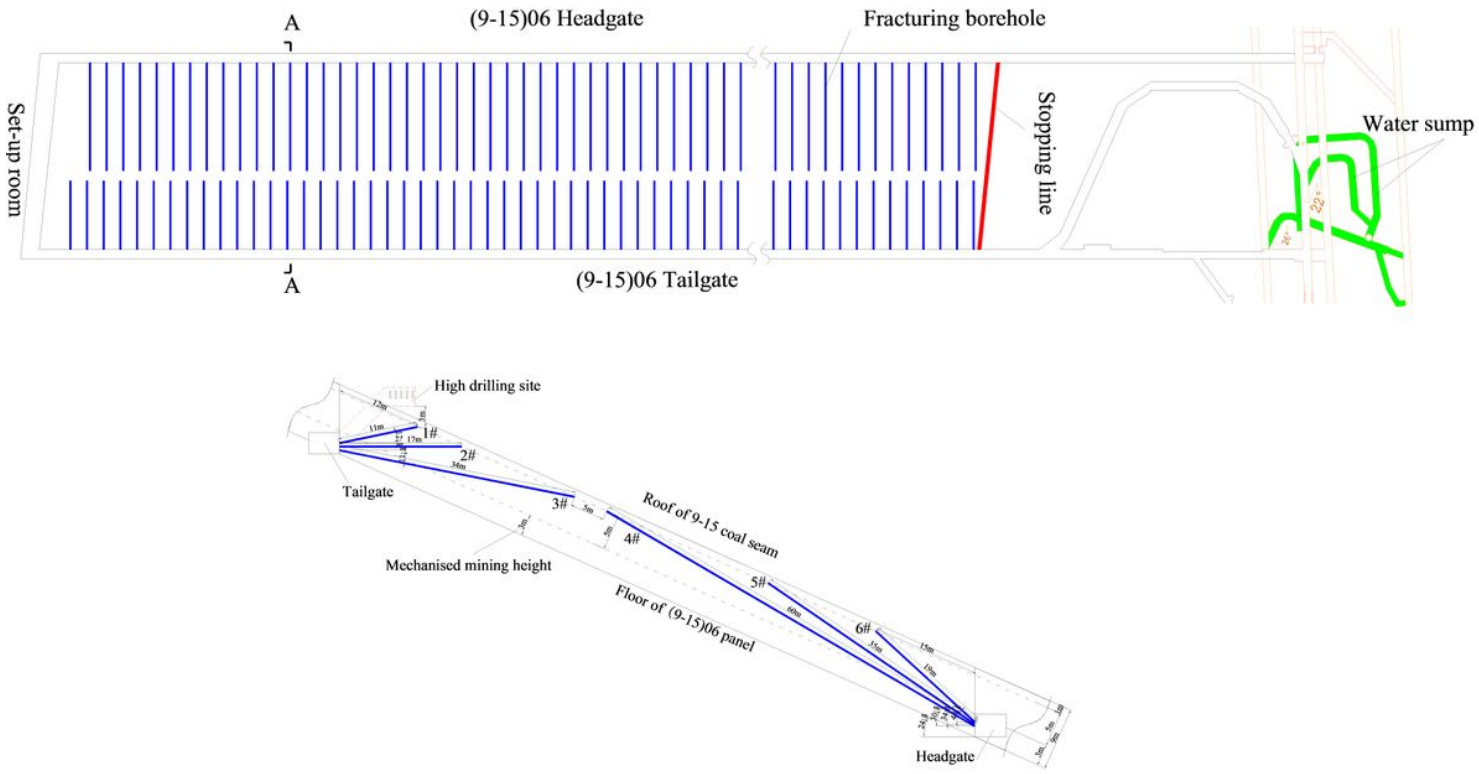

Figure 6

Layout of hydraulic fracturing borehole

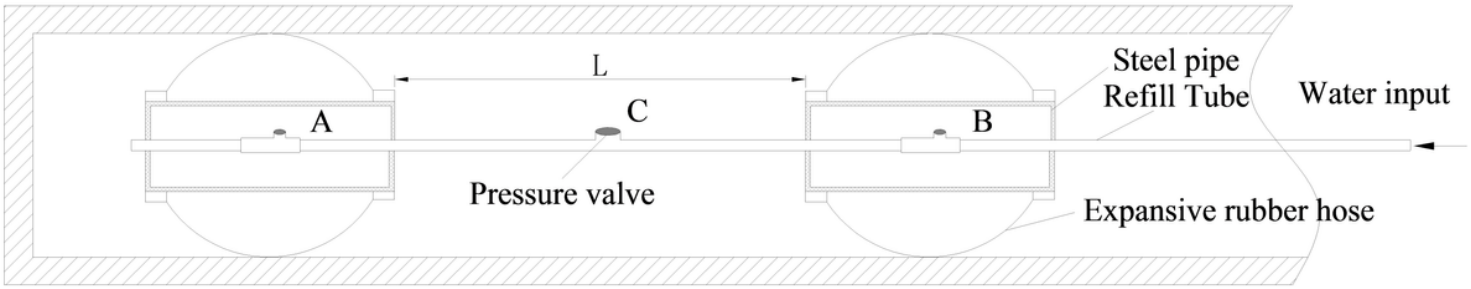

Figure 7

Schematic diagram of sectional sealing

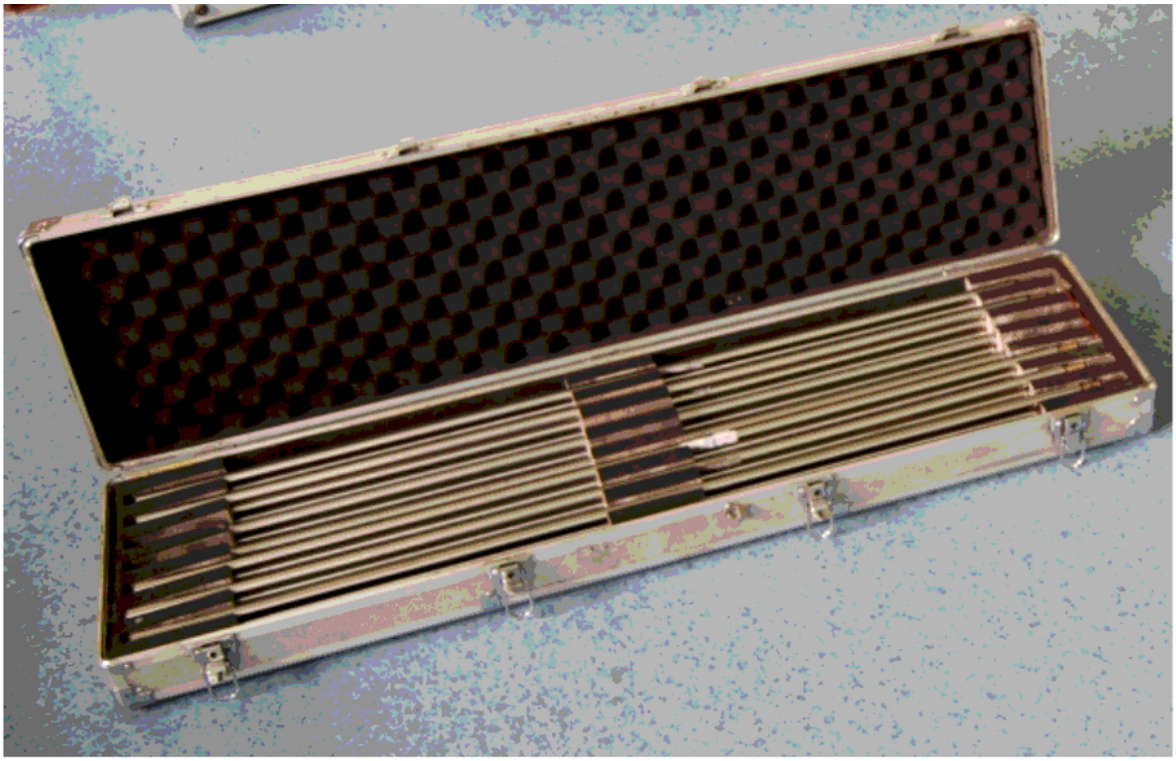

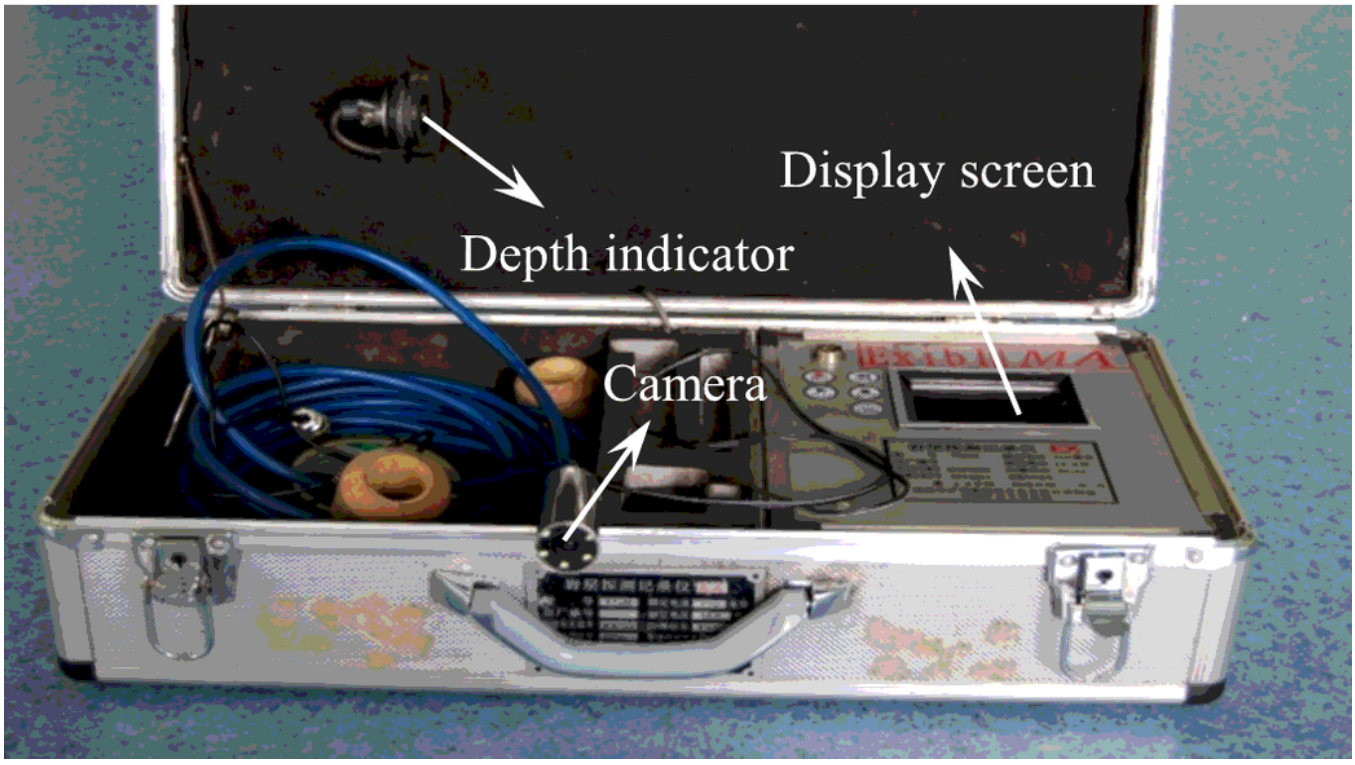

Figure 8

Stratum detector (a) Guide bars (b) Principal machine

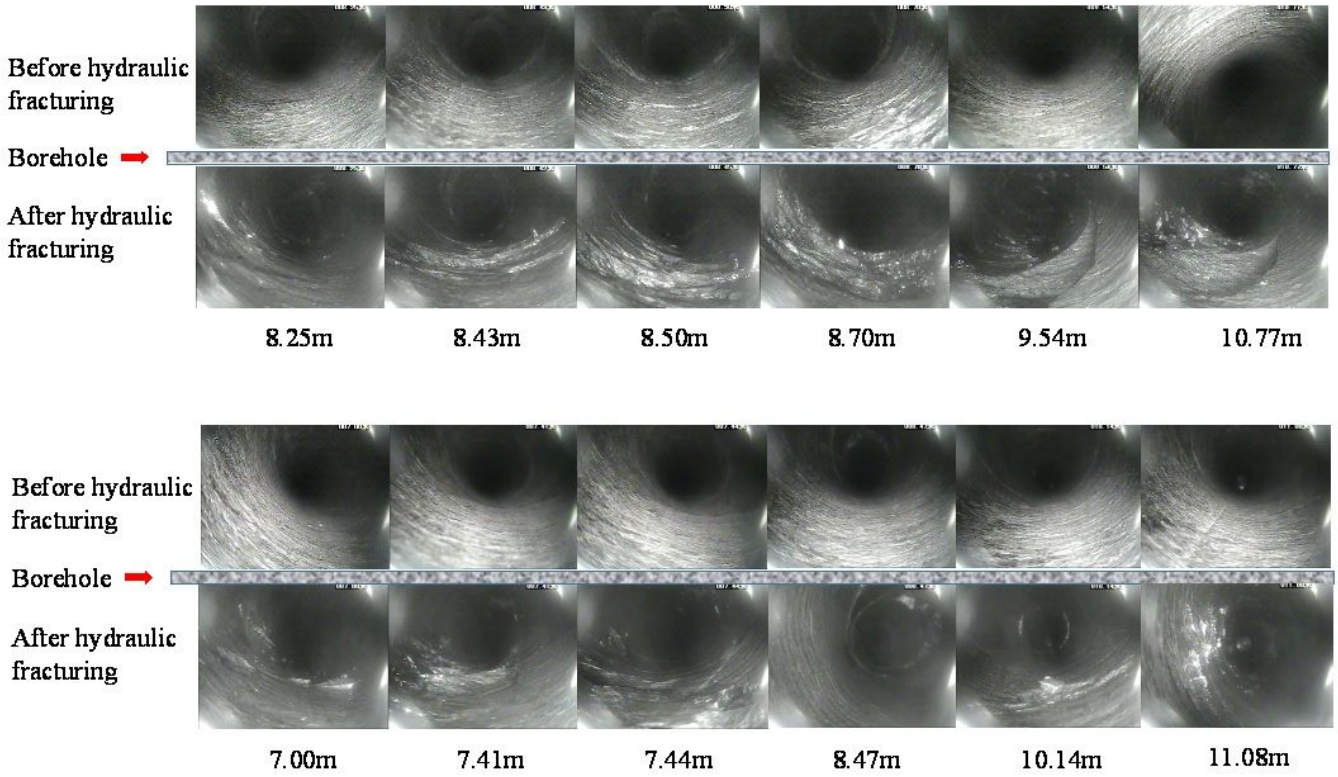

Figure 9

Fracture distribution contrast of part boreholes before and after hydraulic fracturing

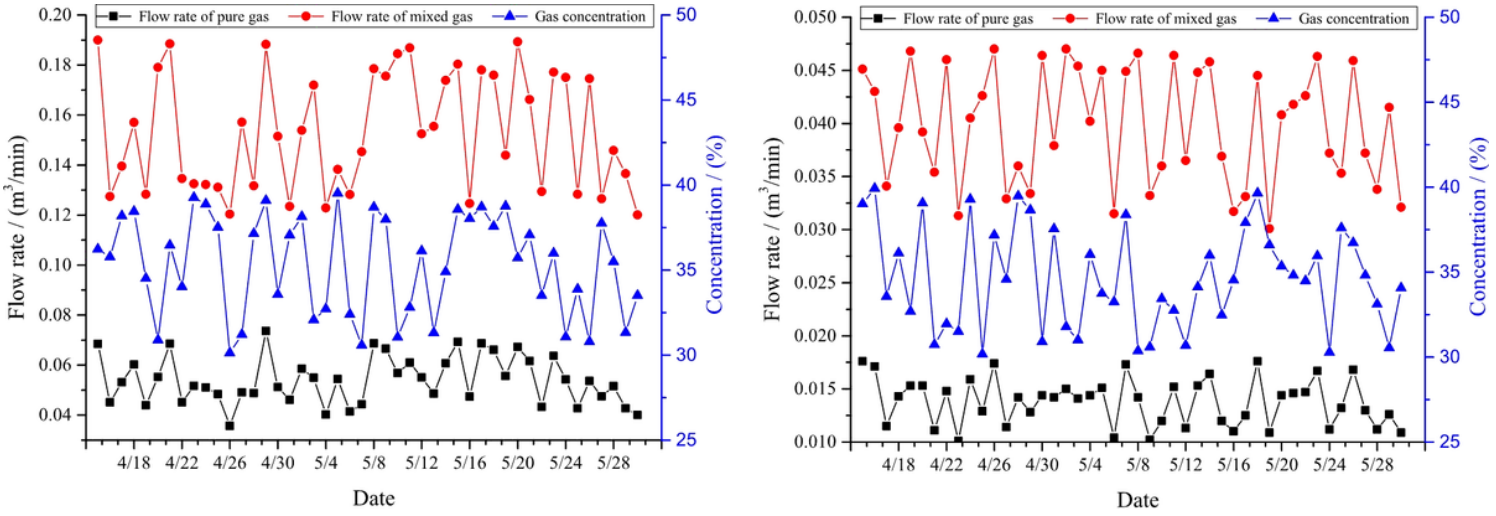

Figure 10

Variation of pre-drainage gas volume of single-hole with time.（a） Borehole after hydraulic fracturing (b） Original borehole

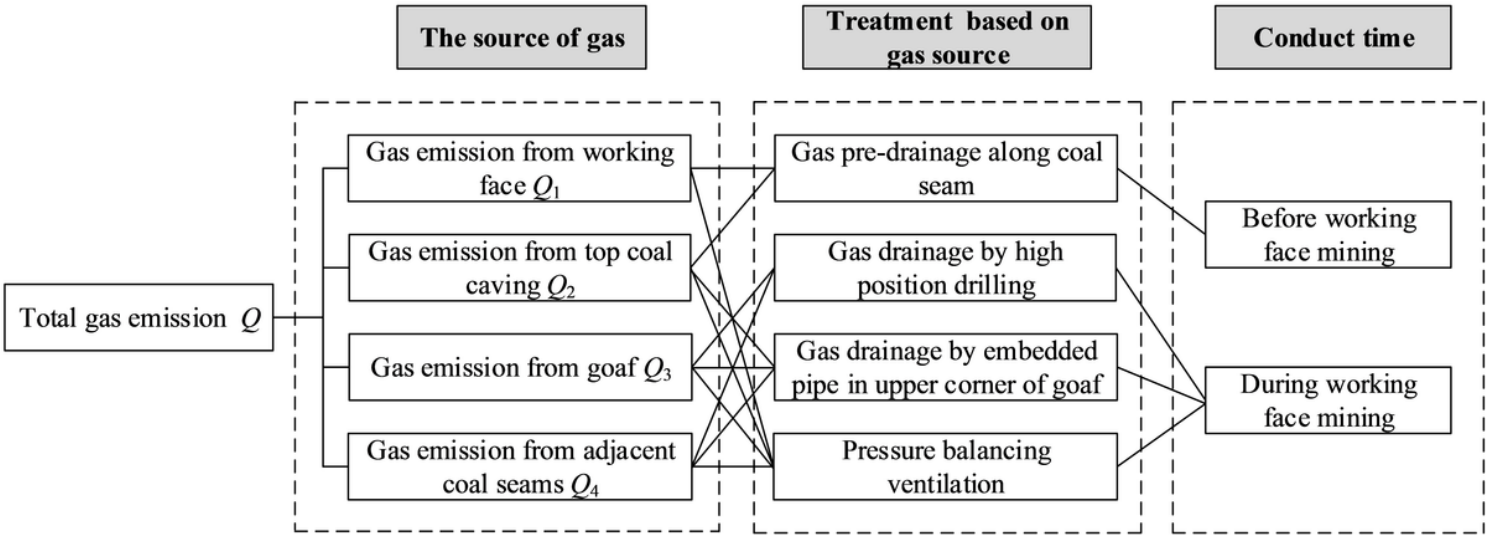

Figure 11

Comprehensive control method based on the sources of gas

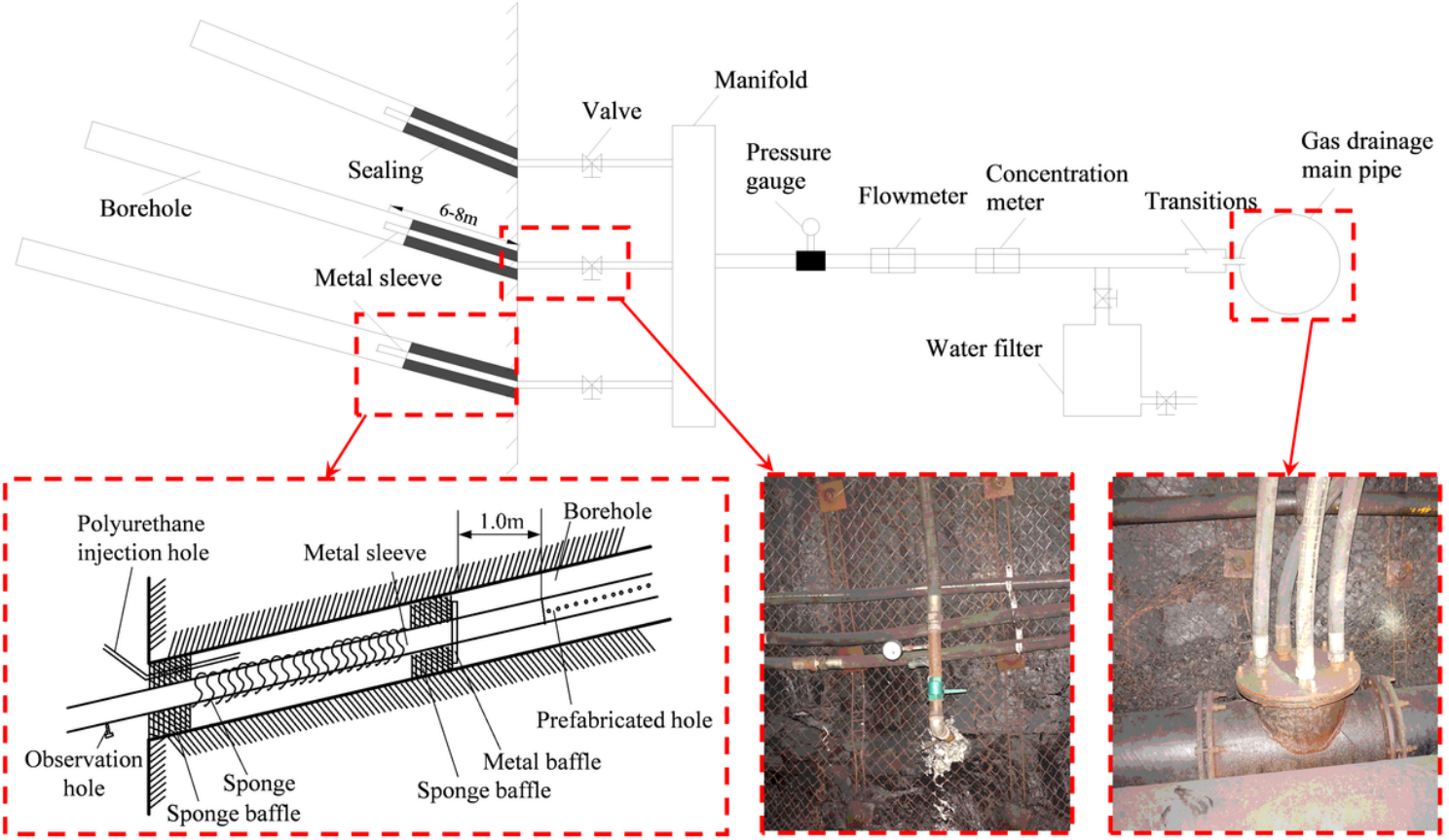

Figure 12

Gas pre-drainage scheme along coal seam

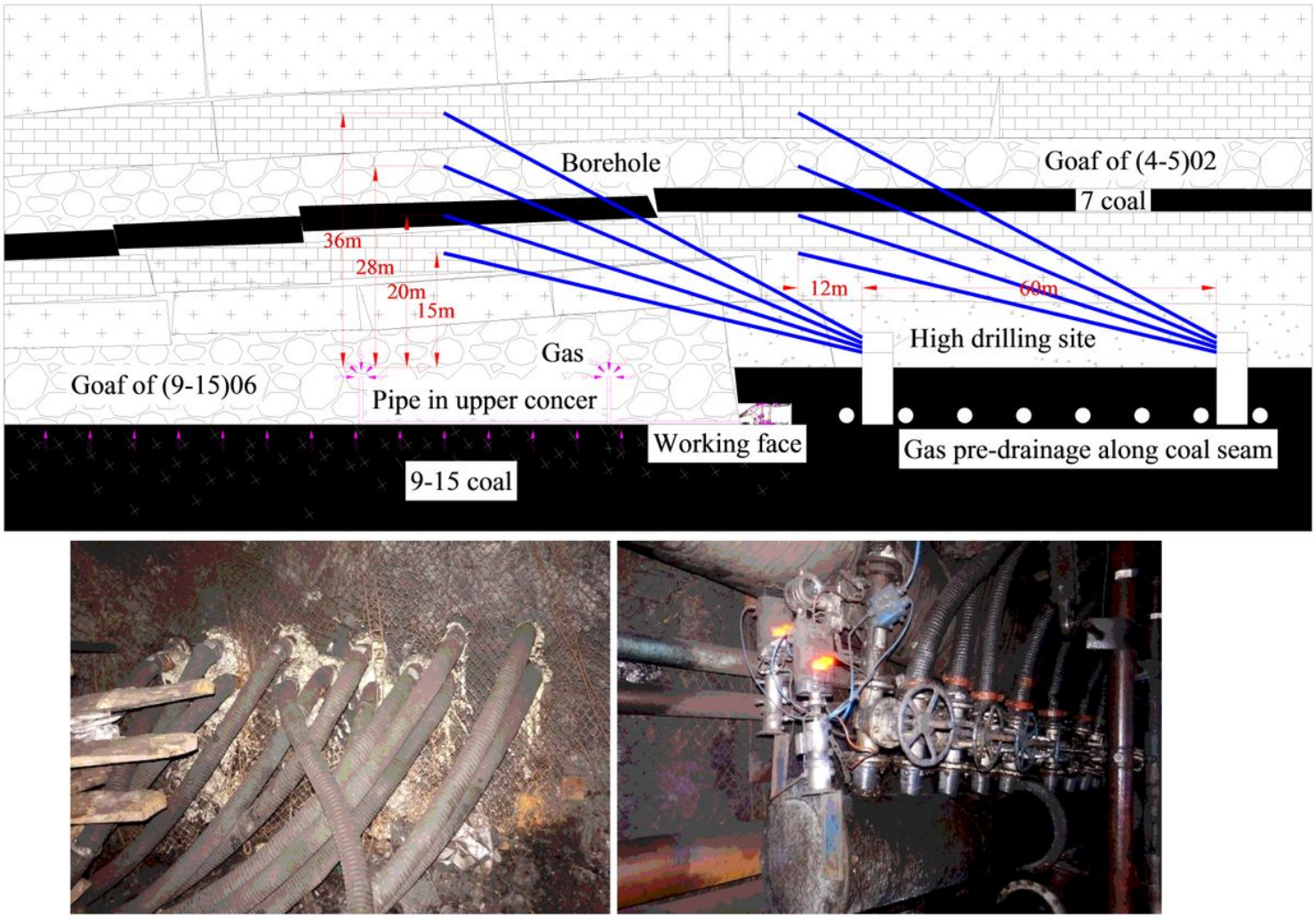

Figure 13

Gas drainage in roof caving zone and fissure zone of (9-15)06 goaf (a) Overburden Structure of (9-15)06 panel and roof high-level gas drainage boreholes (b Boreholes in high drilling site (c Metering installation of gas drainage

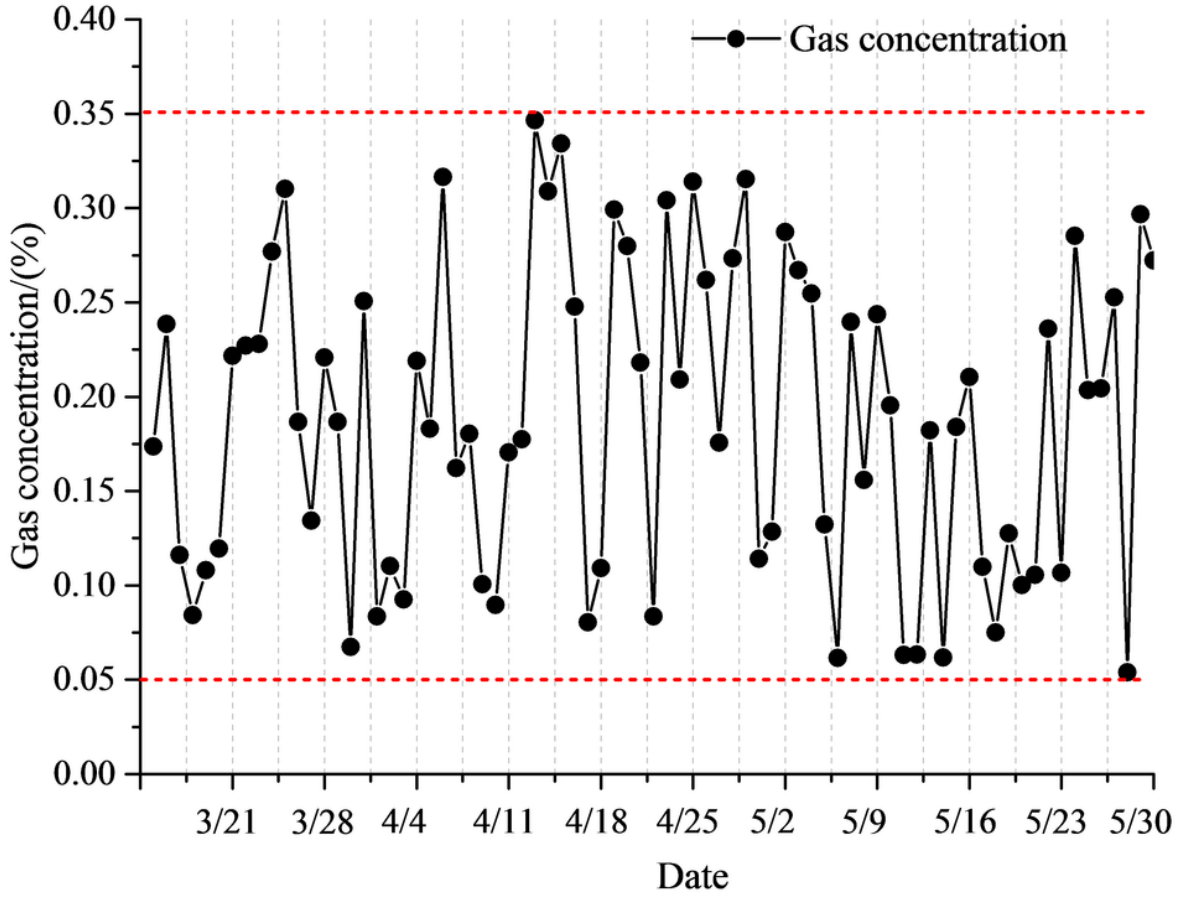

Figure 14

Variation law of gas concentration in return air flow of (9-15)06